

Optical properties of plastically deformed copper: amorphous state with residual nanocrystals

R. RUDOLF^{a,b}, M. GILIĆ^c, M. ROMČEVIĆ^{c,*}, I. ANŽEL^a

^aFaculty of Mechanical Engineering, University of Maribor, 2000 Maribor, Slovenia

^bZlatarna Celje d.d., Kersnikova 19, 3000 Celje, Slovenia

^cInstitute of Physics, University of Belgrade, 11080 Belgrade, Serbia

Chemically pure copper (99.99) prepared in a sample of square cross-section ($10 \times 10 \text{ mm}^2$) and about 50 mm long was extremely plastically deformed with the repeated application of Equal Channel Angular Pressing. AFM investigation gives us information on microstructure with ultrafine grains. The structure of the sample surface, such as the copper oxide and surface roughness over-layer, registered by ellipsometry. Two types of lines are registered by Raman spectroscopy: narrow, with the width $\sim 7 \text{ cm}^{-1}$, and wide ($\sim 40 \text{ cm}^{-1}$), indicates that nano-sized crystal structures related with three dimensional amorphous boundary spaces exist in the specimen.

(Received August 2, 2011; accepted September 15, 2011)

Keywords: Copper, Amorphisation, Atomic force microscopy, Ellipsometric spectroscopy, Raman spectroscopy

1. Introduction

Hydrometallurgical extraction of metals is a branch of industry for which the research work is ongoing to develop processes which cost less, are more environmentally friendly and economically acceptable. Copper is used in a vast variety of products in domestic and industrial domains as a thermal and electrical conductor, and as a constituent of various metal alloys [1]. Among metals, only silver has higher electrical conductivity, but copper is much cheaper and more abundant. Due to this property, copper has been used widely as an electrode in electrochemical studies [2]. Copper is easy to treat, since it is both ductile and malleable. The ease with which it can be drawn into wire makes it useful for electrical work, in addition to its excellent electrical properties. Copper can be machined, although it is usually necessary to use an alloy for complicated parts, such as threaded components, to get really good mixed characteristics. Good thermal conduction makes it useful for heat sinks and in heat exchangers. Copper has good corrosion resistance, but is not as good as gold. It has excellent brazing and soldering properties and can also be welded, although the best results are obtained with gas metal arc welding [3].

The colour of copper samples is usually red or brown due to the existence of thin layers on their surface (including oxide), which are formed gradually when gases (especially oxygen) react with them in the air. Still, the colour of the clean surface is much brighter (pink or bright brown). Copper has its characteristic colour because of its unique band structure. Copper, cesium and gold are the only three elemental metals with a natural colour other than grey or silver [4]. The usual grey colour of metals depends on their "electron sea", which is capable of

absorbing and re-emitting photons over a wide range of frequencies.

In this paper we will present the results of AFM, ellipsometric and Raman spectroscopy measurements of plastically deformed copper.

2. Experimental

2.1. Samples preparation

A chemically pure copper sample (99.99), prepared as a specimen of square cross-section ($10 \times 10 \text{ mm}^2$) and about 50 mm long, was extremely plastically deformed with the repeated application of Equal Channel Angular Pressing (ECAP). ECAP, which is known as one of the discontinuous processes of severe plastic deformation, was applied as an effective technique for producing bulk nano-scaled structures.

The experiments were performed in our experimental hydraulic press (VEB WEMA 250 MP), equipped with a tool for Equal Channel Angular Pressing (ECAP). The tool consists of two intersecting channels of the same cross section ($10 \times 10 \text{ mm}^2$) that meet at the angle $2\Phi = 90^\circ$. The geometry of the tool provides that the material is deformed by simple shear at ideal, frictionless conditions. The cross section of the specimen remains almost equal before and after each step of the process, thus it is possible to subject one specimen to ECAP several times in order to reach high degrees of plastic deformation. In our case, the sample of chemically pure copper was subjected eight times to the ECAP process at room temperature (20°C). This processing, performed at low homologous temperatures, led to a subdivision of the initially coarse grained microstructure into a hierarchical system of cell blocks and

dislocation cells. With increasing strain of the material the size of both of these constituents decreased in size.

2.2. Atomic force microscopy (AFM)

Two samples were prepared for microstructure investigation: Cu 1.1 P- cross section surface, Cu1.2 V- longitudinal section surface. The surfaces of the samples have been investigated using atomic force microscopy (AFM). Fig. 1.a shows a typical picture of a started Cu sample. Figs. 1.b and 1.c show typical topological morphology in two directions (longitudinal and transverse). On the transverse surface more contour particles can be seen, which probably correspond to the nano-sized crystalline phases. Contrary to this, on the longitudinal surface there are essentially less phases, which could be compared to the phases formed on the transverse surface.

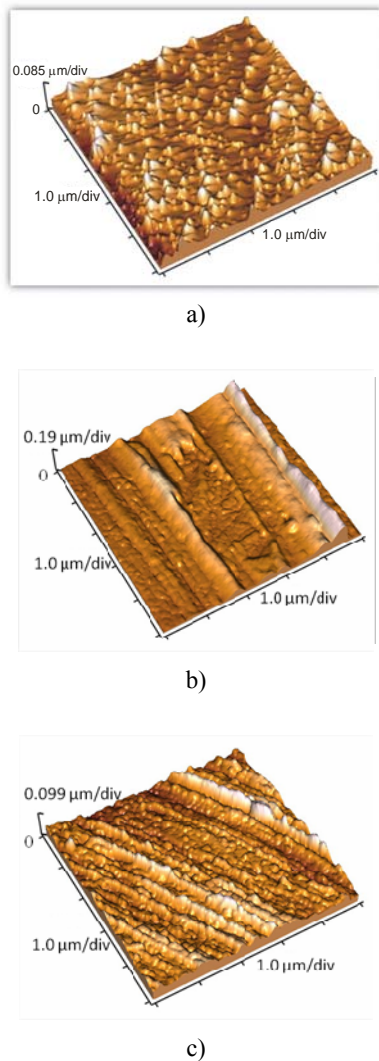


Fig. 1. AFM image of surface of the a) pure Cu; b) Cu1.2 V; c) Cu1.1 P sample.

3. Results and discussion

3.1. Ellipsometric spectroscopy

The ellipsometric measurements were performed using a variable angle spectroscopic ellipsometer (VASE) SOPRA GES5 – IR in the rotating polarizer configuration. The data were collected over the range 1.5 – 4.2 eV with the step of 0.05 eV for three different angles of incidence 65°, 70° and 75°. The 70° angle was chosen for its maximum sensitivity of the ellipsometric data.

The fitting of the model to the experimental data was done using the Levenberg-Marquardt algorithm, to minimize the value of the following merit function [5, 6]:

$$\chi^2 = \frac{1}{2N - P - 1} \sum_{i=1}^N \frac{(\langle \tan(\psi) \rangle_{exp} - \langle \tan(\psi) \rangle_{cal})^2}{\sigma_{1,i}^2} + \frac{(\langle \cos(\Delta) \rangle_{exp} - \langle \cos(\Delta) \rangle_{cal})^2}{\sigma_{2,i}^2} \quad (1)$$

where N is the total number of data points, P is the number of fitted parameters, $\langle \tan(\psi) \rangle_{exp}$, $\langle \tan(\psi) \rangle_{cal}$ and $\langle \cos(\Delta) \rangle_{exp}$, $\langle \cos(\Delta) \rangle_{cal}$ represent the experimental and calculated values of ellipsometric quantities $\tan(\psi)$ and $\cos(\Delta)$, and σ_i is the error of each measured quantity. All calculations were made using Winelli_II, Version 2.0.0.0.

Spectroscopic Ellipsometry (SE) is a surface-sensitive, non-destructive optical technique used to characterize surface changes, optical constants of bulk or layered materials, over-layer thicknesses, multilayer structures, and surface or interface roughness [6]. Ellipsometry measures $\tan(\psi)$ and $\cos(\Delta)$ spectra which are, respectively, the amplitude and projected phases of the complex ratio:

$$\rho = r_p / r_s = \tan(\psi) e^{i\Delta} \quad (2)$$

where r_p and r_s are the complex reflectance coefficients of light, polarized parallel (p) and perpendicular (s) to the plane of incidence, respectively. Ellipsometric quantities ψ and Δ are sensitive to changes of different parameters such as surface conditions, over-layer structure, dielectric function of the material and others.

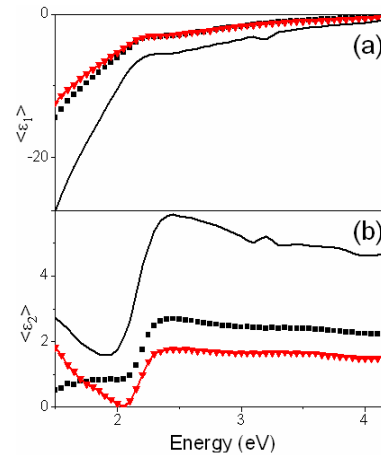


Fig. 2. (a) Real and (b) imaginary part of pseudo-dielectric function for Cu1.1P (squares), Cu1.2 V (triangles) and bulk copper (solid line).

When it is exposed to oxygen copper oxidizes naturally to copper (I) oxide (Cu_2O). The influence of the surface roughness also has to be taken into account. Fig. 2 presents both real and imaginary parts of pseudo-dielectric function for the bulk copper and samples Cu1.1P and Cu1.2V. Therefore, the ellipsometric spectra ($\tan(\psi)$, $\cos(\Delta)$) of the two samples Cu1.1P and Cu1.2V were fitted using a two-film model: Cu as a substrate, an over-layer of Cu_2O and a surface-roughness layer, Fig. 3.c. The surface roughness over-layer is composed of the bulk copper oxide and an ambient. Using Bruggeman effective medium approximation [6], we calculated the volume fraction of the constituents.

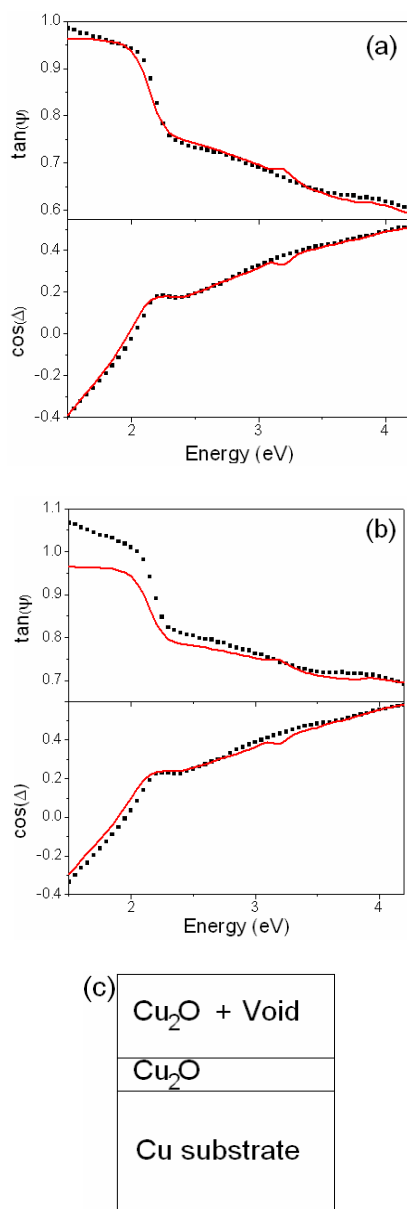


Fig. 3. (a) Experimental data (dots) and fitted data (solid line) of the sample Cu1.1P; (b) experimental data (dots) and fitted data (solid line) of the sample Cu1.2V; (c) sketched model.

Fig. 3a presents the experimental and the best fitting data of the sample Cu1.1P. The thickness of the Cu_2O is ~ 1.5 nm, and the roughness over-layer, with 80% of Cu_2O and 20% of void, is ~ 25.6 nm. For the energies above 2 eV this fit is better than for the energies around and below this value. This may indicate that the dielectric function of the sample substrate is different from the one of the bulk copper taken from Palik [7], and that these changes are due to plastic deformation.

The best fit to the model of the sample Cu1.2V is presented in Fig. 3b. The thickness of the copper oxide is ~ 1.7 nm, and the roughness over-layer, with 81% of the oxide and 19% of the void, is ~ 35 nm. Comparing these two fits one can see that, in the case of the Cu1.1P sample, the model with Cu_2O and surface roughness is better suited than in the case of the Cu1.2V sample.

3.2. Raman spectroscopy

The micro-Raman spectra were taken in the backscattering configuration and analyzed by Jobin Yvon T64000 spectrometer, equipped with nitrogen cooled charge-coupled-device detector. As an excitation source we used the 514.5 nm line of an Ar-iron laser. The measurements were performed at different laser power.

Pure copper, in principle crystallized in the face centered cubic type structure (O_h space group symmetry), and the first order Raman modes are not active. However, plastic deformation of the sample as well as penetration of oxygen into the sample (and creating CuO), causes the appearance of Raman active modes. Factor group analysis for CuO yields [8]:

$$\text{Cu}(C_2): \Gamma = 3A_u + 3B_u, \quad (3)$$

$$\text{O}(C_2): \Gamma = A_g + 2B_g + A_u + 2B_u, \quad (4)$$

$$\Gamma_{\text{CuO}} = A_g + 2B_g + 4A_u + 5B_u. \quad (5)$$

Of these modes, $1A_u(T_y)$ and $2B_u(T_x, T_z)$ are acoustical modes, so that the total of vibrational modes ($\mathbf{q} = 0$) and their activity is:

$$\Gamma_{\text{CuO}}^{\text{vib}} = A_g(R) + 2B_g(R) + 3A_u(ir) + 3B_u(ir) \quad (6)$$

Thus, three Raman (A_g, B_g) and six infrared (A_u, B_u) active modes are to be expected in the spectra of CuO.

The Raman spectra of Cu1.2V and Cu1.1P are presented in Figs. 4 and 5. In addition to a very narrow line (with a width of ~ 2 cm^{-1}), two types of lines are clearly visible in the spectra: narrow (~ 7 cm^{-1}) and wide (~ 40 cm^{-1}) lines. To demonstrate the nature of these very narrow lines in the range up to 120 cm^{-1} , the spectrum of nitrogen is given on the insert of Fig. 4. It is obvious that the positions of these narrow lines from the insert match corresponding lines registered in the spectrum on Fig. 4. and Fig. 5. So it can be concluded that they are the parasite lines. The narrow lines are well defined, so we used the de-convolution method in analysis of the wide lines. Raman scattering spectra are often analyzed with the help

of a Lorentzian function, or by the convolution of a Lorentzian and Gaussian curves [9]. As the quality of the spectra in Figs. 4 and 5 is such that it allows only a qualitative analysis with a partial discussion of the trend, we assumed that all lines are of the Lorentzian type. A typical line shape obtained in this way is also shown in Figs. 4 and 5. Dashed lines correspond to the Rayleigh scattering and luminescence [10]. Well resolved peaks appear at about 98, 150, 162 and 220 cm^{-1} for the sample Cu1.2V (Fig. 4) and at 98 and 150 cm^{-1} are observed for the sample Cu1.1P (Fig. 5). Differences in the spectra originated from the different deformation.

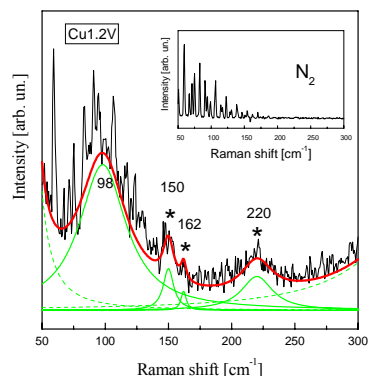


Fig. 4. Raman spectra of Cu1.2 V sample. Inset: Raman spectra of N_2 .

Narrow lines, which are marked by stars in Fig. 4, originated from the crystal structures Cu and CuO. The appearance of CuO modes, as we have already said, is a consequence of the oxygen penetration in the sample. The registered lines originate from Cu-Cu and Cu-O [8]. The wide line is a consequence of the amorphous state. Namely, the wide line at 98 cm^{-1} originated from CuO that became amorphous. In this range, the CuO phonon states density is large [8], and therefore the line is no longer narrow.

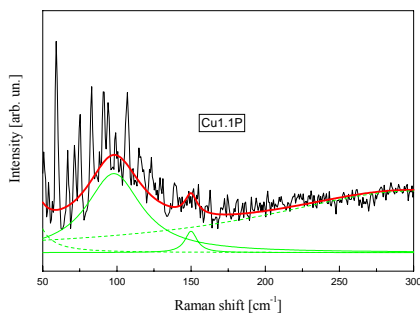


Fig. 5. Raman spectra of Cu1.1 P sample.

The mode at 220 cm^{-1} is probably a consequence of the multi-phonon process. The absence of those structures in the Cu1.1P Raman spectra points to the influence of material treatments on the structure of Cu and CuO. The existence of two types of lines indicates that nano-sized crystal structures of both Cu and CuO related with three dimensional amorphous boundary spaces exist in the specimen, which indicates that the plastic deformation of

the sample did not lead to total amorphisation of the specimen.

4. Conclusion

The results are presented of the AFM, ellipsometric and Raman measurements of plastically deformed copper. The three layer model was used to calculate the thickness of spontaneously formed copper oxide and surface roughness (ellipsometric measurements). It is shown that this model is better suited for microstructure investigation of the sample Cu 1.1 P-cross section surface than for the Cu1.2 V-longitudinal section surface. Two types of lines: narrow (with width of $\sim 7 \text{ cm}^{-1}$) and wide ($\sim 40 \text{ cm}^{-1}$), are registered by Raman spectroscopy. The existence of two types of lines indicates that nano-sized crystal structures of both Cu and CuO related with three dimensional amorphous boundary spaces exist in the specimen. The obtained results indicated that the plastic deformation of the sample did not lead to total amorphisation of the specimen.

Acknowledgments

This work was supported under the Programme of Scientific and Technological Cooperation between the Republic of Slovenia and the Republic of Serbia. Work in Serbia is supported by the Serbian Ministry of Education and Science (Project 45003). This paper is part of the Slovenian MNT ERA-NET Project no. 3211-07-000023: Nano Structured Metal Ceramic Composites.

References

- [1] N. Habbache, N. Alane, S. Djerad, L. Tifouti, *Chemical Engineering Journal*, **152**, 503 (2009).
- [2] G. Karim-Nezhad, R. Jafarloo, P. Seyed Dorraji, *ElectrochimicaActa*, **54**, 5721 (2009).
- [3] W. F. Smith, J. Hashemi, *Foundations of Materials Science and Engineering*. (2003).
- [4] Chambers, William; Chambers, Robert, *Chambers's Information for the People.L* (5th ed.). W. & R. Chambers. (1884).
- [5] M. Losurdo, *Thin Solid Films* **455–456**, 301 (2004).
- [6] R. M. A. Azzam, N. M. Bashara, *Ellipsometry and Polarized Light*, North-Holland, Amsterdam (1977).
- [7] E. D. Palik, *Handbook of Optical Constants of Solids*, Academic Press, USA (1985).
- [8] G. Kliche, Z. V. Popovic, *Phys. Rev. B*, **42**, 1060 (1990).
- [9] Z. Ž. Lazarević, S. Kostić, M. J. Romčević, J. Trajić, B. Hadžić, D. Stojanović, N. Ž. Romčević, *Optoelectron. Adv. Mater. – Rapid Commun.* **5**(2), 150 (2011).
- [10] B. N. Henry, in: J.R. Doring (Ed.), *Raman Spectroscopy: Sixty Years On*, vol. **10**, Elsevier, Amsterdam (2008).

*Corresponding author. romcevic@ipb.ac.rs